Absent anisotropy: The paradox of the Southern Alps orogen

Anna Pulford, Martha Savage, and Tim Stern
Victoria University of Wellington, New Zealand

Received 16 May 2003; revised 31 July 2003; accepted 5 September 2003; published 24 October 2003.

[1] A high resolution active source dataset recorded across the Southern Alps of New Zealand displays unusually strong S-wave phases, which show minimal shear wave splitting. A suite of methods was used to analyse the data to minimize the uncertainty in the anisotropy measurements. We use the *Silver and Chan* [1991] method, cross correlation of stacked data, and deconvolution in combination with the other methods. The results were consistent at each station, but differed between stations. Fault-parallel fast directions with delay times of 0–0.08 s were calculated from the most impulsive S-wave arrivals. The crustal rocks from the Southern Alps are strongly anisotropic in the laboratory, contrasting with results shown here. The minimal delay times suggest that the shear waves are affected by multiple phases of deformation in the crust. *INDEX TERMS:* 7205 Seismology: Continental crust (1242); 8010 Structural Geology: Fractures and faults; 8102 Tectonophysics: Continental contractional orogenic belts; 8110 Tectonophysics: Continental tectonics—general (0905); 8150 Tectonophysics: Plate boundary—general (3040). **Citation:** Pulford, A., M. Savage, and T. Stern, Absent anisotropy: The paradox of the Southern Alps orogen, *Geophys. Res. Lett.*, *30*(20), 2051, doi:10.1029/2003GL017758, 2003.

1. Introduction

[2] Seismic anisotropy identified by shear wave splitting of SKS phases in New Zealand shows some of the largest delay times in the world (2 sec) [*Klosko et al.*, 1999]. SKS splitting is often ascribed purely to mineral alignment of the mantle. Under New Zealand strong Pn anisotropy of at least 10 ± 3% has been reported from both the South [*Scherwath et al.*, 2002] and North Islands [*Kayal and Smith*, 1984]. The crustal component of this splitting signal is unknown, but highly anisotropic schists [*Okaya et al.*, 1995; *Godfrey et al.*, 2000] near the surface in the Alpine Fault region indicate that crustal anisotropy could contribute to the SKS delay times. A high resolution active source seismic experiment recorded across the Southern Alps (1996 South Island GeopHysical Project) (Figure 1) [*Stern et al.*, 1997], which recorded strong shear wave arrivals, enable us to investigate the crustal component of splitting.

2. Anisotropy Theory

[3] Seismic anisotropy occurs when seismic waves travel through a medium that has directional variations in velocity. These variations result from the alignment of minerals, such as olivine crystals in the mantle [*Silver and Chan*, 1991], structural alignment of fault rocks and re-mineralization fabrics [e.g., *Okaya et al.*, 1995] and pervasive orientations of cracks in the uppermost crust [*Crampin*, 1994; *Miller and Savage*, 2001]. The effect of oriented cracks rapidly decreases with depth as the cracks are closed by pressure and mineral alignment becomes the major source of seismic anisotropy [*Crampin*, 1994; *Godfrey et al.*, 2000].

[4] Anisotropy can result in shear wave splitting, in which shear waves polarized in one direction (fast direction ϕ) travel faster than another. The time lag between the fastest arrival and the slower phase, polarized orthogonally, is the delay time (δt).

3. Crustal Structure Under the Southern Alps

[5] The collisional boundary between the Pacific and Australian plates is marked by the Alpine Fault, which runs obliquely across South Island (Figure 1). A change in the pole of rotation at 6.4 Ma resulted in a change from predominantly strike-slip motion along the Alpine Fault to transpression, including 80–100 km of shortening and 230 km of dextral shear [*Walcott*, 1998]. This change in plate motion vector coincides with the postulated timing of rapid uplift of the Southern Alps, which run parallel to the plate boundary.

[6] In central South Island the Alpine Fault appears at small scales to be a single strike slip fault. On a scale of 1–10 km, however, the fault is a complex series of oblique thrust segments joined by right-lateral sub-vertical faults [*Norris and Cooper*, 1995]. The structure of the Southern Alps is complex with several phases of overprinted deformation [*Little et al.*, 2002]. Three main deformation phases may influence S-wave anisotropy in the crust: 1) an early phase, which was originally sub-horizontal and is likely to have the least effect as it is overprinted by later deformation; 2) the main Haast schist foliation, which is thought to decrease in dip eastward away from the Alpine Fault; and 3) vertical shearing, recorded as brittle-ductile shears, which allows the Alpine Fault rocks to be exhumed towards the surface in a step-like fashion [*Wellman*, 1979] as recorded by the rocks that have passed through the brittle-ductile zone [*Little et al.*, 2002].

[7] The Haast schist foliation and the brittle-ductile shears are both close to vertically aligned near the surface and may have similarly oriented anisotropy symmetry axes, enhancing the anisotropy. As seismic waves reflect or refract towards the surface they are oriented approximately parallel to the foliation, which would result in shear wave splitting with ϕ aligned with the transverse component (048°, radial 318°). However, at depth the dip of the Alpine Fault zone is thought to become more horizontal [*Kleffmann et al.*, 1998; *Scherwath et al.*, 2002], while the brittle-ductile shear bands are thought to remain close to vertical [*Little et al.*, 2002], which might change the resultant anisotropy.

0094-8276/03/2003GL017758$05.00

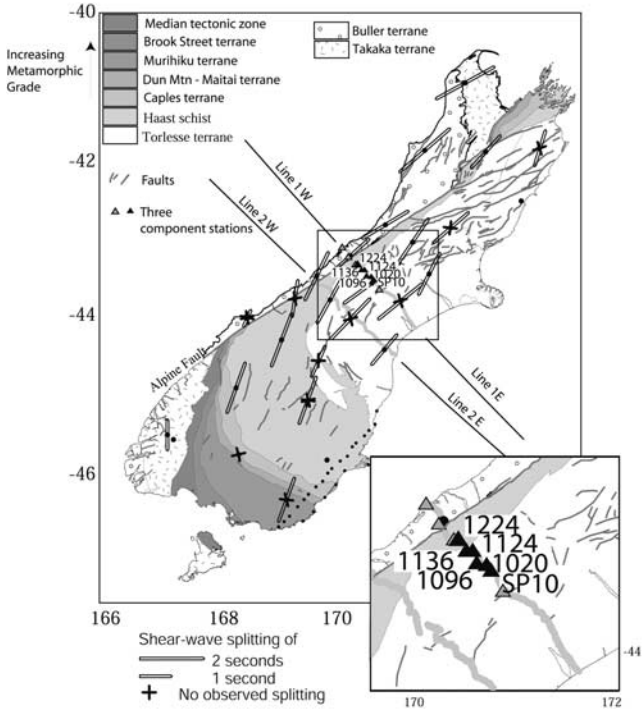

Figure 1. Geology of the South Island and geometry of the South Island GeopHysical Transect (SIGHT). Bars outlined in black indicate ϕ and δt (bar length) determined from SKS results [*Klosko et al.*, 1999], short black bars indicate a null result. Locations showing both short and long bars have recorded different results from waves arriving from different directions. Triangles indicate the location of three component stations utilised during the firing of Line 1W of the SIGHT project. Black triangles are stations used in this study. Grey dots indicate the location of 1 and 2 component seismometers used in the SIGHT project. Lines 1W, 1E, 2E, and 2W are the ship tracks for the firing of an airgun array, recorded by the three component stations. The inset shows the detail of station locations.

[8] Laboratory measurements of samples of Haast schist and mylonitic rocks collected from the surface across the Southern Alps show strong P and S-wave anisotropy (max ~17%) [*Okaya et al.*, 1995; *Godfrey et al.*, 2000]. Variations in the angle of wave propagation relative to the foliation of the schist have a greater influence on measured anisotropy than metamorphic grade, with speeds varying between 5 and 7 km/s for P-waves and 2.5 and 4 km/s for S-waves [*Godfrey et al.*, 2000].

4. Anisotropy Analysis

[9] Few studies have reported crustal shear wave splitting from active source experiments due to the weak, emergent nature of S-wave phases and lack of 3 component recorders. Three component receivers, located across South Island collinear with, and recording shots from, Line 1W of the 1996 SIGHT project [*Stern et al.*, 1997], record strong S-wave arrivals over a range of offsets and appear ideal for S-wave splitting analysis. Due to the absence of a standard method with which to analyse these short wavelength data, we employ a range of methods. These include the *Silver and Chan* [1991] method created for analysis of long wavelength earthquake source phases, cross correlation of stacked seismic data and deconvolution.

5. Silver and Chan Method

[10] The method of *Silver and Chan* [1991] was employed to calculate ϕ, δt and the initial polarization (ϕ_i) of the S-wave prior to splitting. The results were graded A (good)-D (poor) based on linearity of particle motion after correction for splitting and uniqueness of solution. Only the A results were analysed further. These results show strong variations in ϕ_i and δt between different stations and offsets (Figure 2a). The dataset was re-analysed with ϕ_i set to the radial direction (318°), assuming that ϕ_i of the incoming wave would be aligned along the line from the shots to the stations. P-wave arrivals reflected off the Moho show a back azimuth of 331 ± 12°. Setting ϕ_i to radial improved the quality of the result. To test whether radial ϕ_i provides the optimal results, the initial polarization was varied systematically over a 180° range (Figure 2b).

[11] Delay times are consistent at ~0.05 s despite variations in both ϕ and ϕ_i. This value is in agreement with that

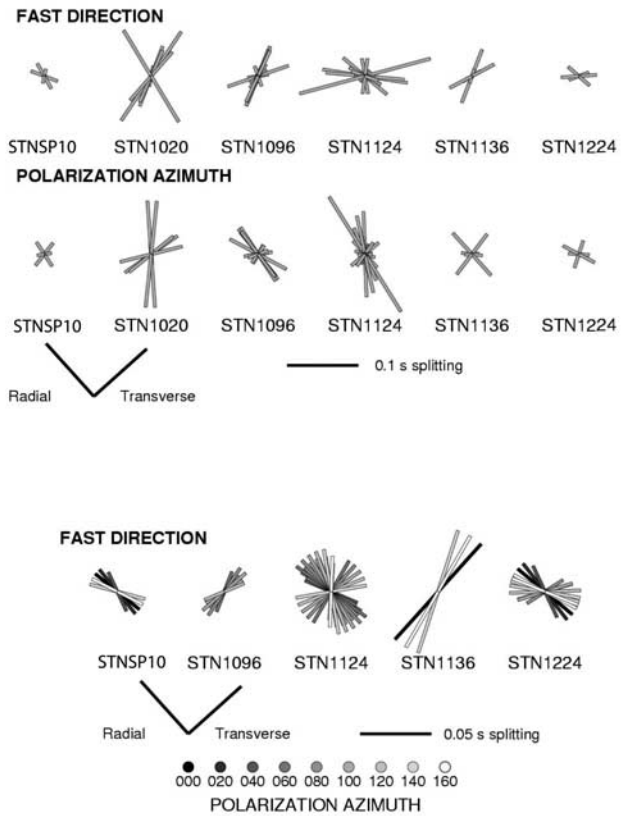

Figure 2. (a) Fast orientations from the *Silver and Chan* [1991] method. Grid north is aligned vertically up the page, the radial and transverse directions are shown. (b) Results of Silver and Chan method with fixed ϕ_i. The bars are scaled by δt and shaded according to the value to which ϕ_i was set. Only A graded results are shown; they can be achieved over a range of ϕ_i, resulting in a range of ϕ. Constraining ϕ_i through particle motion analysis, increases certainty in the results of this method.

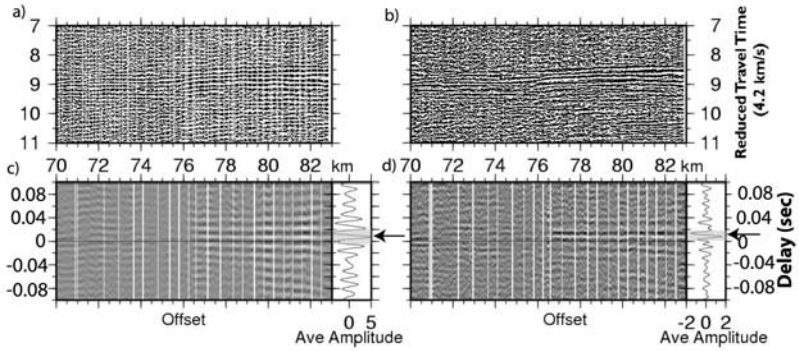

Figure 3. Cross correlation of radial (318°) and transverse component (048°) recording of SmS arrivals into stn1136. (a) SmS arrival recorded on the radial component. (b) SmS arrival shown in a) after deconvolution of the data with a Wiener predictive filter (gap length of 1.08 s and filter length of 6.20 s). (c) Cross correlation of the radial (318°) and transverse (048°) components. The darkest and lightest grey indicate strong correlation and mid grey shows poor correlation. Positive delay times show that the transverse direction is the fast direction and negative values that the radial is the fast direction. (d) Cross correlation of the deconvolved horizontal components. In (c) and (d) the graph at the end of the plot is the average amplitude for all offsets, which is used to identify the best delay time (greatest amplitude, here shaded in light grey and highlighted with an arrow). In (d) the amplitude graph shows a best fit for 0.08 s or 0.14 s delay with the transverse component fast.

determined without fixing ϕ_i and is equal to about 1/2 the period. This indicates that cycle skipping may be occurring due to the emergent nature of the first arrivals. Cycle skipping occurs when the corrected waveform is mis-correlated by a multiple of half or one cycle of the data; this is often a problem for high frequency data. The average of the best results is $\phi = 291 \pm 48°$ and $\phi_i = 99 \pm 48°$. Broadly it appears that ϕ of stnSP10 and stn1224 are aligned in the radial direction, stn1096 and stn1136 in the transverse direction and stn1124 appears to show no splitting. The best results have ϕ_i aligned approximately radially (138–318°), as expected.

6. Cross-Correlation

[12] Radial and transverse components from stn1096, stn1124 and stn1136 (Figure 3a) were cross-correlated using a cross covariance equation to calculate δt. We identified the most likely δt by the largest amplitude of cross-correlation (darkest or lightest grey) over a range of offsets, and also by the amplitude of the trace of average cross correlation (Figure 3c). The emergent, multiple, nature of the data has resulted in the waveforms correlating well over a range of δt. Therefore, cross-correlation results from stations stn1096, stn1124 and stn1136 (Figure 3c) are non-unique with the most likely δt between 0.06 s with the radial component fast, or 0.12 s with the transverse component fast.

7. Deconvolution

[13] Deconvolution is generally used on near vertical active source stacked datasets to reduce the number of multiples and reverberations. The aim is to compress the seismic wavelet into a spike [*Yilmaz*, 1987]. Deconvolution assumes that each new seismic wave arriving at the station will arrive at a random time and that only multiples in the data will have the same wavelength.

[14] Deconvolution was applied to data from stations stn1096, stn1124 and stn1136 (Figures 3a and 3b). This process reduced the number of multiples, but the data retained an emergent waveform. The deconvolved traces were analysed using the *Silver and Chan* [1991] method and the cross-correlation method. Results of the Silver and Chan method on the deconvolved data are consistent with those presented earlier; ϕ is aligned with the transverse orientation for stn1096 and stn1136. Stn1124 shows an approximately northward oriented ϕ, which is better constrained than that obtained from the data prior to deconvolution. Cross-correlation (Figure 3d) of the deconvolved data (Figure 3b) shows a reduced range of possible δt and more certainty that ϕ is aligned with the transverse component. Using the amplitude of the trace showing the average deconvolved cross-correlation (Figure 3d), the best δt for stn1096 are 0.04 and 0.09 s, 0 and 0.06 s for stn1124 and 0.08 and 0.14 s for stn1136. The lower values, for each station, show marginally stronger correlation.

[15] Deconvolution improves the certainty of δt and confirms the presence of splitting. However, deconvolution can change the frequency of the data. It is assumed here that the shear wave arrival recorded on the two horizontal components will have the same wavelength but be delayed by δt. Deconvolution will correct both components in the same manner if they are identical. If the two components differ in original frequency content, or arrivals on one component are not seen on the other, the deconvolution will correct each of the waveforms in a different way resulting in the increased possibility of incorrect cross-correlation.

8. Discussion

[16] Shear wave splitting of 0–0.08 s, with the fast direction aligned with the transverse component (approximately parallel with the plate boundary), is identified from active source seismic data with raypaths travelling across the plate boundary between the Pacific and Australian Plate. The strong transverse component observed in the SIGHT dataset is likely sourced from either reflection off the anisotropic mantle or passage through the Alpine Schist, and hence the transverse energy is likely to be created on the upward ray path [*Guest and Thomson*, 1992]. If the trans-

verse component energy is created through reflection off the mantle, then the recorded splitting of 0.08 s corresponds to a minimum of 0.025% anisotropy. A delay time of 0.08 s is approximately 4% of the 2 s SKS splitting.

[17] The crustal rocks of the Southern Alps demonstrate strong shear wave splitting when analysed in a laboratory [*Okaya et al.*, 1995; *Godfrey et al.*, 2000] and hence the results of this experiment are unexpected. The geometry of the experiment and ray paths relative to the foliation plane and structure of the Southern Alps may be a contributing factor to the small observed δt. Laboratory measurements by *Godfrey et al.* [2000] have shown that where the shear waves pass normal to the foliation plane of the schist rocks (0° to the symmetry axis), both the radial and transverse components are inhibited by the same amount, resulting in no apparent splitting. A singularity also occurs when the shear waves are passing through the schist foliation at ~50° to the symmetry axis [*Godfrey et al.*, 2000], also resulting in no splitting. In the Southern Alps the foliation of the mylonites and schist close to the Alpine Fault are measured to be close to vertical and are thought to decrease in dip with depth, towards the east. Waves passing through this package of rocks arrive obliquely at the surface. Particle motions of Pg and PmP arrivals were estimated (an allowance for the free surface was made) and the incident angles of arrival ranged from 12–20°.

[18] The angle of incidence to the symmetry axis would need to vary from 48° at STN1096 to 50° at STN1124 and back to 48° at STN1136 to fit the observed (low) splitting at these stations, which invokes unrealistic orientations of the Alpine Fault zone at depth given the angle of incidence of the incoming waves [*Godfrey et al.*, 2000].

[19] A second possible contributing factor to the low splitting values is that there are several phases of deformation recorded by these rocks [*Little et al.*, 2002] and each of these may have some influence on the anisotropy. Rocks exhumed at the surface that passed through the brittle-ductile zone show repeated veining and fractures. These fractures are approximately 30 cm apart, crop out over a region of several kilometres and are thought to record the step-like uplift of the rocks [*Wellman*, 1979; *Little et al.*, 2002]. These features are roughly parallel to the Alpine Fault but dip vertically and in some cases towards the Alpine Fault [*Little et al.*, 2002]. Although these fractures are only preserved in the brittle-ductile region, the stresses causing these features will affect the whole of the Southern Alps. If both the mineral alignment of the schist and the fracture alignment of the brittle-ductile transition zone influence the shear wave splitting, then the oblique nature of the two structures may cause any splitting to be cancelled at some stations while others may still record splitting. However, this would require a slightly different angle of ray path, or small scale variations in structure orientation, below each station.

9. Summary

[20] Shear wave splitting analysis for the crust of the Southern Alps indicate 0–0.08 s of splitting with the transverse (fault-parallel) component being the fast direction. Consistent results are obtained using both single trace methods of *Silver and Chan* [1991] and stacked data methods. The best results are obtained using a combination of deconvolution and cross correlation on stacked data.

[21] Low or zero delay times for the crust are unexpected, as these rocks have been shown to be strongly anisotropic when measured in the laboratory [*Godfrey et al.*, 2000]. These low delay times are most likely the result of multiple phases of deformation [*Little et al.*, 2002], which formed differently oriented structures to produce destructive interference and obscure or cancel any splitting that might result from a single phase of deformation. Either slight differences in the angle of the ray path through the anisotropic rocks for each station, or spatial variations in anisotropy on the scale of 1 km are needed to produce the observed variations in delay time. Finally, the strong anisotropy observed in the laboratory is made from small samples that cannot emulate the structures over a wide region and hence may be unrealistically high.

[22] **Acknowledgments.** We thank D. Okaya and K. Gledhill for valuable comments. NSF, FRST, the Marsden Fund, and a Victoria University of Wellington Targeted Scholarship provided funding. Fieldwork for this project was undertaken by the members of the 1996 SIGHT working group.

References

Crampin, S., The fracture criticality of crustal rocks, *Geophys. J. Int.*, *118*, 428–438, 1994.

Godfrey, N. J., N. I. Christensen, and D. A. Okaya, Anisotropy of schists: Contributions of crustal anisotropy to active source seismic experiments and shear wave splitting observations, *J. Geophys. Res.*, *105*(B12), 27,991–28,007, 2000.

Guest, W. S., and C. J. Thomson, A source of significant transverse arrivals from an isotropic-anisotropic interface, e.g., the Moho, *Geophys. J. Int.*, *111*, 309–318, 1992.

Kayal, J. R., and E. G. C. Smith, Upper mantle P-wave velocities in the south east North Island, New Zealand, *Tectonophys.*, *104*(1)–(2), 115–125, 1984.

Kleffmann, S., F. Davey, A. Melhuish, D. Okaya, T. Stern, and the SIGHT Team, Crustal structure in the central South Island, New Zealand, from the Lake Pukaki seismic experiment, *New Zealand J. Geol. Geophys.*, *41*, 39–49, 1998.

Klosko, E. R., F. T. Wu, H. J. Anderson, D. Eberhart-Phillips, T. V. McEvilly, E. Audoine, M. K. Savage, and K. R. Gledhill, Upper Mantle Anisotropy in the New Zealand region, *Geophys. Res. Lett.*, *26*(10), 1497–1500, 1999.

Little, T. A., R. J. Holcombe, and B. R. Ilg, Kinematics of oblique continental collision inferred from ductile microstructures and strain in mid-crustal Alpine Schist, central South Island, New Zealand, *J. Struct. Geol.*, *24*, 219–239, 2002.

Miller, V., and M. Savage, Changes in seismic anisotropy after volcanic eruptions: Evidence from Mount Ruapehu, *Science*, *293*, 2231–2233, 2001.

Norris, R. J., and A. F. Cooper, Origin of small-scale segmentation and transpressional thrusting along the Alpine Fault, New Zealand, *Bull. Geol. Soc. Am.*, *107*, 231–240, 1995.

Okaya, D., N. I. Christensen, D. Stanley, and T. Stern, Crustal anisotropy in the vicinity of the Alpine Fault zone, South Island, New Zealand, *New Zealand J. Geol. Geophys.*, *38*, 579–583, 1995.

Scherwath, M., A. Melhuish, T. Stern, and P. Molnar, Pn anisotropy and distributed upper mantle deformation associated with a continental transform fault, *Geophys. Res. Lett.*, *29*(8), 16-1–14-4, 2002.

Silver, P. G., and W. W. Chan, Shear-wave splitting and subcontinental mantle deformation, *J. Geophys. Res.*, *96*, 16,429–16,454, 1991.

Stern, T. A., P. E. Wannamaker, D. Eberhart-Phillips, D. Okaya, and F. J. Davey, Mountain building and active deformation studied in New Zealand, *EOS Trans. Am. Geophys. Union.*, *78*, 329, 335–336, 1997.

Walcott, R. I., Modes of oblique compression: Late Cenozoic tectonics of the South Island of New Zealand, *Reviews Geophys.*, *36*(1), 1–26, 1998.

Wellman, H. W., An uplift map of South Island, New Zealand, and a model for uplift of the Southern Alps, *Roy. Soc. New Zealand Bull.*, *18*, 1979.

Yilmaz, O., *Investigations in Geophysics, Seismic Data Processing*, Series 2, pub: Society of Exploration Geophysics, 1987.

A. Pulford, M. Savage, and T. Stern, Victoria University of Wellington, New Zealand. (anna_pulford@yahoo.com.au)